Supplementary Materials: Naphthyl-Containing Organophosphonate Derivatives of Keggin-Type Polyoxotungstates

Nerea Andino, Beñat Artetxe, Santiago Reinoso, Pablo Vitoria, Leire San Felices, Jose I. Martínez, Fernando López Arbeloa and Juan M. Gutiérrez-Zorrilla

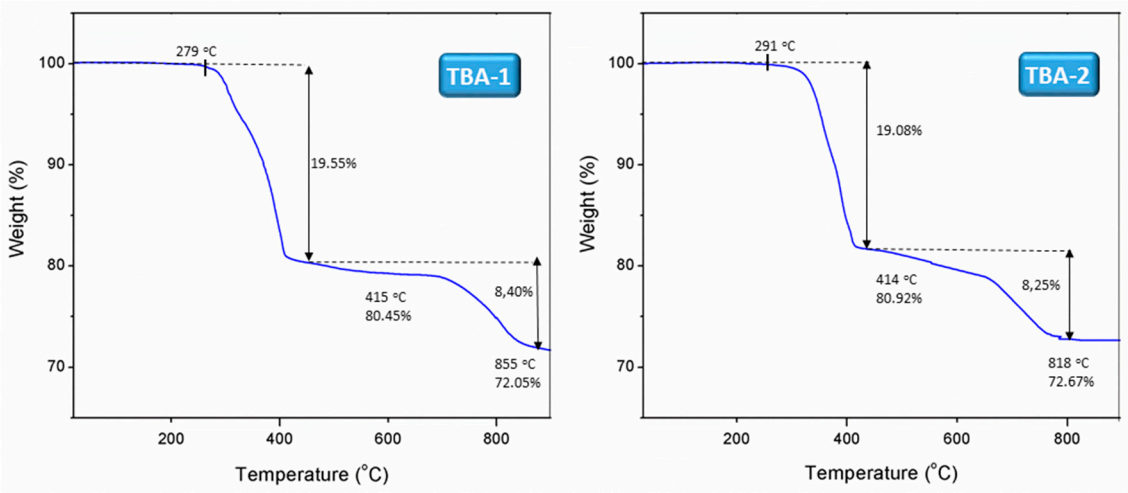

Figure S1. TGA curves for **TBA-1** and **TBA-2**.

Table S1. Bond lengths (Å) and angles (°) for the P atoms in **TBA-1** and **TBA-2**.

Atom	P–C	P–O_{POM1}	P–O_{POM2}	P–O_T	<P–C–C>
TBA-1					
P1	1.80(2)	1.514(16)	1.520(13)	1.533(17)	114.1(16)
P2	1.88(2)	1.498(15)	1.535(18)	1.51(2)	109(3)
P21	1.83(3)	1.522(17)	1.528(14)	1.530(18)	109.4(19)
P22	1.88(3)	1.562(17)	1.570(19)	1.499(18)	108(2)
TBA-2					
P1	1.81(5)	1.56(2)	1.585(16)	1.504(18)	109(3)
P2	1.75(4)	1.548(16)	1.532(14)	1.479(17)	109(2)
P21	1.77(3)	1.547(19)	1.526(14)	1.507(16)	107(2)
P22	1.76(4)	1.56(2)	1.535(16)	1.485(17)	111(3)

Table S2. Geometrical parameters (Å, °) for the intermolecular C–H···O hydrogen bonds involving 1-naphthylmethylphosphonate groups and O_{POM} atoms in **TBA-1** and **TBA-2**.

D–H···A	H···A	D···A	<D–H···A>
TBA-1			
C8–H8···O223	2.57	3.30(3)	133
C8–H8···O229	2.52	3.39(3)	152
C9–H9···O207	2.55	3.48(4)	169
C29–H29···O209 [i]	2.42	2.966(17)	116
C208–H208···O14 [ii]	2.66	3.30(3)	126
C208–H208···O15 [ii]	2.60	3.37(4)	138
C208–H208···O20 [ii]	2.97	3.58(3)	123
C209–H209···O3 [ii]	2.57	3.50(4)	167
C209–H209···O14 [ii]	2.98	3.50(3)	116
C229–H229···O11 [iii]	2.54	3.02(5)	112
TBA-2			
C9–H9···O211 [iv]	2.35	2.98(4)	124
C28–H28···O214	2.70	3.388(16)	129
C28–H28···O215	2.79	3.553(16)	138
C28–H28···O220	2.96	3.599(15)	125
C29–H29···O203	2.44	3.38(3)	167
C208–H208···O14 [ii]	2.66	3.364(15)	131
C208–H208···O15 [ii]	2.91	3.569(15)	127
C208–H208···O20 [ii]	2.78	3.529(16)	137
C209–H209···O1 [ii]	2.46	3.387(16)	165
C229–H229···O10 [v]	2.23	2.87(4)	124

Symmetry codes: (i) $-x, 3-y, 1-z$; (ii) $x, -1+y, z$; (iii) $1-x, 3-y, 1-z$; (iv) $2-x, -y, 1-z$; (v) $1-x, -y, 1-z$.

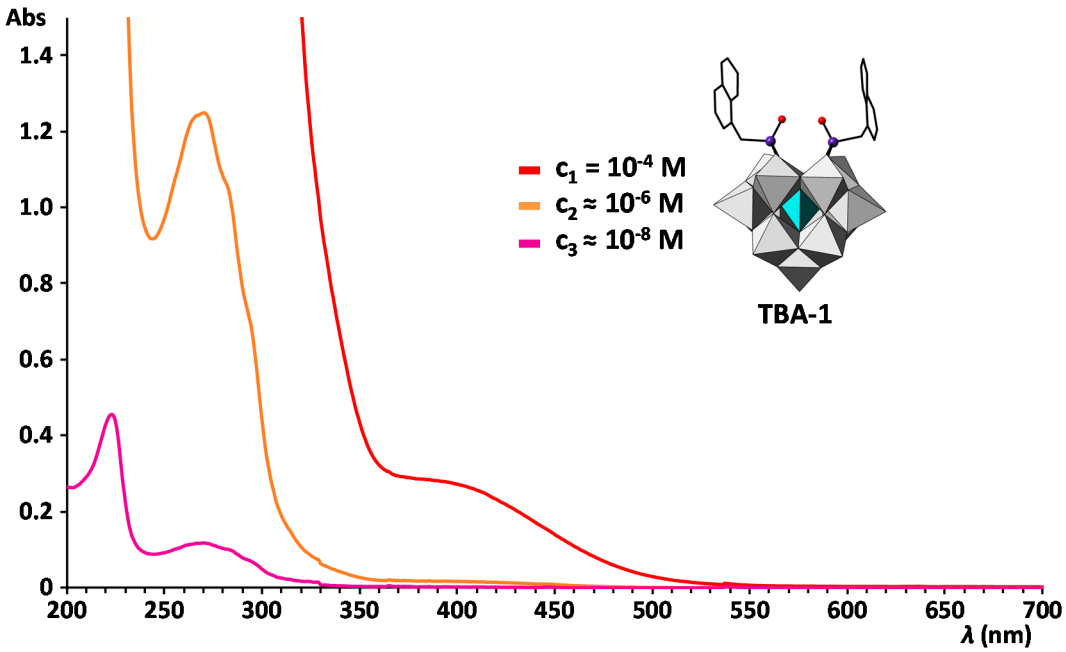

Figure S2. UV–Vis spectra of acetonitrile solutions of **TBA-1** with different concentrations.

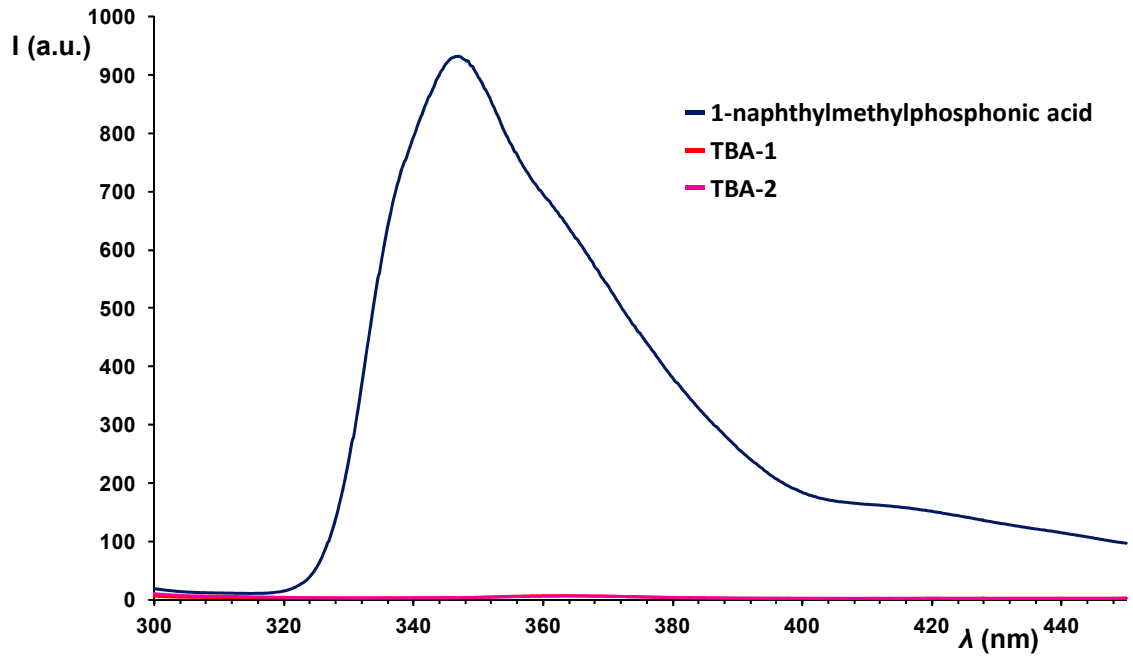

Figure S3. Fluorescence emission spectra of solid samples of **TBA-1**, **TBA-2** and 1-naphthylmethylphosphonic acid in the 300–450 nm region (λ_{exc} = 283 nm).

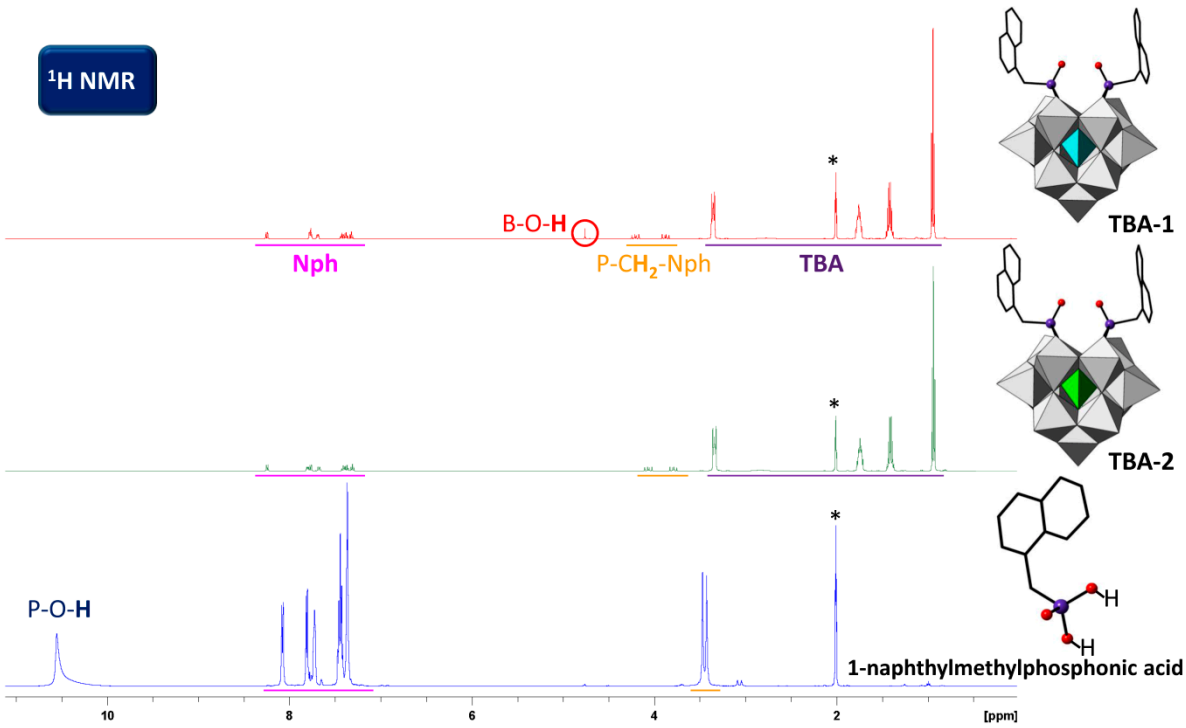

Figure S4. ^{1}H-NMR spectra of **TBA-1** and **TBA-2** in acetone-d_6 compared with that of the commercial 1-naphthylmethylphosphonic acid. The signals labeled as * correspond to the non-deuterated acetone.

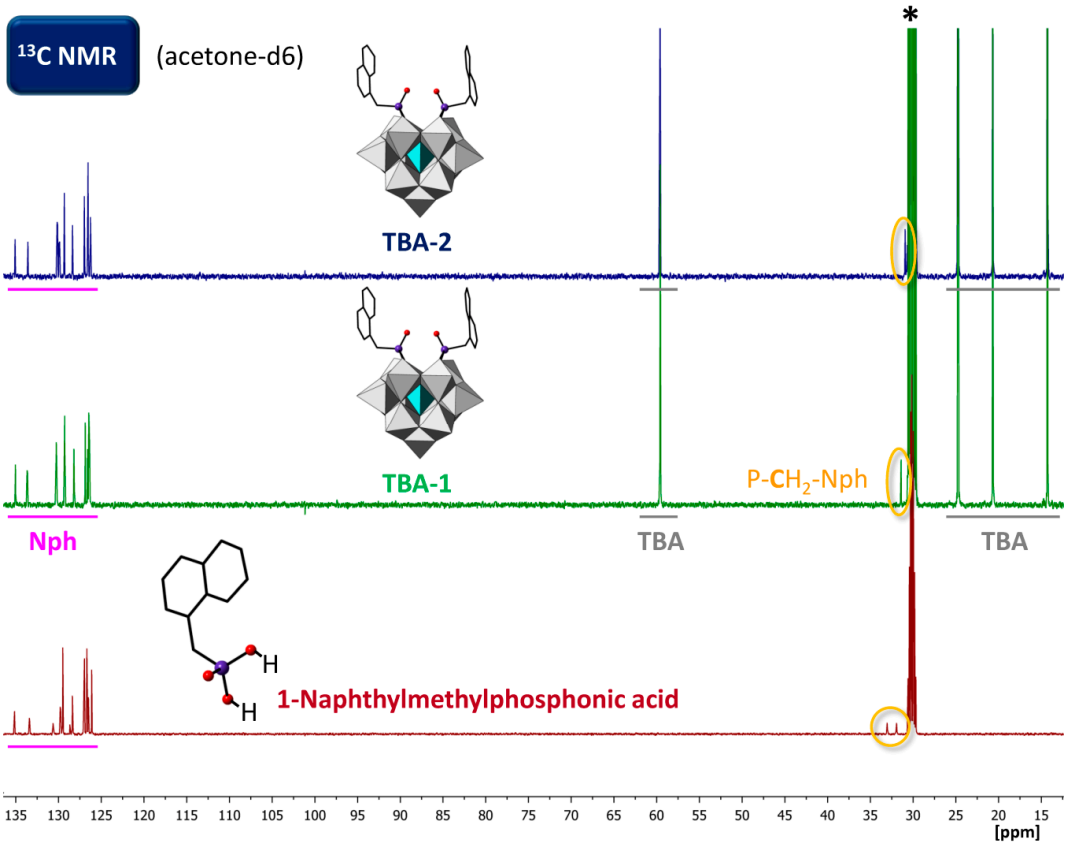

Figure S5. ^{13}C-NMR spectra of **TBA-1** and **TBA-2** in acetone-d_6 compared with that of the commercial 1-naphthylmethylphosphonic acid. The signals labeled as * correspond to the solvent.

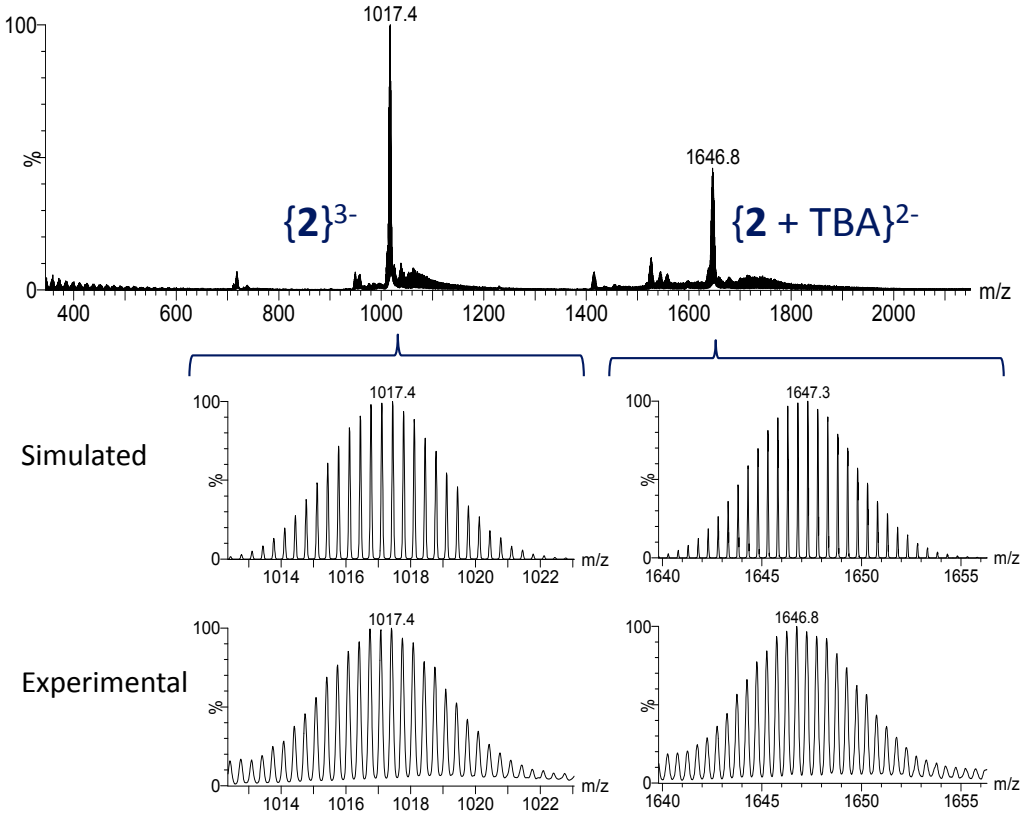

Figure S6. Negative ESI mass spectrum of a CH_3CN solution of **TBA-2** (U_c = 15 V) and comparison of the signals corresponding to the species $\{\mathbf{2}\}^{3-}$ = $[H(C_{11}H_9PO)_2(SiW_{11}O_{39})]^{3-}$ and $\{\mathbf{2}$ + TBA$\}^{2-}$ = $\{(C_{16}H_{36}N)[H(C_{11}H_9PO)_2(SiW_{11}O_{39})]\}^{2-}$ with the simulated isotopic patterns.